Effect of Volume Translation on Two-Phase Equilibrium Calculations for Hydrocarbon Mixtures in a Confined Space

by

Wenran Zhao

A thesis submitted in partial fulfillment of the requirements for the degree of

Master of Science

in

Petroleum Engineering

Department of Civil and Environmental Engineering

University of Alberta

ABSTRACT

Oil production from tight/shale reservoirs has drawn an increasing attention over the past decades. One of the essential mechanisms affecting the oil/gas production is the phase behavior of the reservoir fluids in the confined nanopores inside the tight/shale reservoirs. Many theoretical works couple the conventional multiphase flash calculation procedure with capillary pressure to study the phase equilibrium of reservoir fluids in nanopores. However, the most widely used Peng-Robinson equation of state (PR-EOS) (Peng and Robinson, 1976), which is applied in the conventional multiphase flash calculations, does not provide an accurate prediction on liquid-phase density. This inherent flaw of PR-EOS weakens the reliability of the calculation algorithm developed to study the phase equilibrium in nanopores because the incorrect phase density prediction leads to incorrect vapor-liquid interfacial tension predictions. Capillary pressure, which relies on vapor-liquid interfacial tension, is thereby calculated with poor accuracy. This work aims to address this issue by developing a new two-phase equilibrium calculation algorithm that couples capillarity effect and volume translation in the conventional multiphase flash calculation. In this work, PR-EOS together with the volume translation method proposed by Abudour *et al.* (2012) is applied to more accurately predict liquid-phase density. Vapor-liquid interfacial tension is calculated using the Weinaug-Katz model (Weinaug and Katz, 1943). The Young-Laplace equation (Young, 1805) is used to calculate capillary pressure with assumptions of zero contact angle and equal principle radii. Phase behavior of two mixtures in confined nanopores is studied to examine the accuracy and robustness of the two-phase flash algorithm developed in this work. For each mixture, two-phase envelope is calculated using the algorithm developed in this work

and the calculated results are then compared with experimental data collected from the literature. It is observed that, at a fixed temperature, the bubble point and dew point pressures of the two mixtures in nanopores are reduced due to capillary pressure compared to those under bulk condition. After the phase densities are corrected by the volume translation method, the bubble point and dew point pressures are reduced to a larger extent at a fixed temperature. Compared to the two-phase flash algorithm without the use of volume translation, the two-phase flash algorithm with the use of volume translation gives a better match to the measured dew point pressures.

DEDICATION

This dissertation is dedicated to my dearest parents: Mrs. Honghong Shan and Mr. Dongye Zhao.

ACKNOWLEDGMENTS

I would like to express my gratitude for the support and guidance provided by my supervisor Dr. Huazhou Li. I would also like to thank my committee members, Dr. Nobuo Maeda, and Dr. Yang Liu for their constructive comments and suggestions made on my thesis.

I greatly acknowledge the following individuals and organizations for their support during my study at the University of Alberta:

- My past and present members in Dr. Li's research group;
- Faculty and staff in the Department of Civil and Environmental Engineering at the University of Alberta.

TABLE OF CONTENTS

LIST OF TABLES

LIST OF FIGURES

CHAPTER 1 INTRODUCTION

1.1. Research Background

A precise description of the reservoir fluids phase behavior is of prime consideration for reservoir simulations in the oil and gas industry. Multiphase flash calculations are normally employed to provide information on phase equilibrium of reservoir fluids. The most commonly used tool in the multiphase flash calculations is cubic equation of state (CEOS). A CEOS, such as the PR-EOS (Peng and Robinson, 1976), describes the volumetric behavior of the reservoir fluid system by requiring only the critical properties and acentric factor of each component. Although CEOSs were initially developed for pure components, they can be used to multicomponent systems when a certain mixing rule is utilized. Conventional multiphase flash calculations can output mole fractions and compositions of the equilibrium phases at a given temperature, pressure, and overall composition.

In tight/shale reservoirs, however, the conventional multiphase flash calculation is no longer valid. The nanopores found in tight/shale reservoirs introduce large capillary pressure, which significantly alters the phase equilibrium of reservoir fluids. The existence of capillary pressure in nanopores causes an imbalance between vapor-phase pressure and liquid-phase pressure. In this case, reservoir fluids show phase behavior different from what is predicted by classic thermodynamics. Numerous attempts have been made to theoretically investigate the effect of capillary pressure on the multiphase equilibrium of reservoir fluids in confined nanopores. One of the most straightforward methods is using the EOS based model. This

method considers the pressure difference between the adjacent phases by solving for the phase mole fractions, compositions and capillary pressures simultaneously. The resulted fluid phase equilibrium yielded by this method is different from that under bulk condition and are more representative in describing the phase behavior of the reservoir fluids in confined nanopores.

Multiphase flash calculation coupled with capillary pressure relies on phase densities calculated from CEOS. However, liquid-phase density is often less accurately predicted by the CEOS. Since the genesis work of Martin (1979), many volume translation (VT) methods have been proposed to improve the accuracy of density prediction by CEOS. The methods developed afterward ranged from simple constant correction terms (Peneloux *et al.*, 1982) to more complex temperature or density dependent models (Watson *et al.* 1986; Chou and Prausnitz, 1989; Magoulas and Tassios, 1990; Tsai and Chen, 1998; Ahlers and Gmehling, 2001; Lin and Duan, 2005; Baled *et al*., 2012; Abudour *et al*., 2012; Abudour, *et al.*, 2013; Shi *et al*., 2018). One important aspect of a consistent volume translation method is that the application of this method leaves the predicted equilibrium conditions unchanged (Peneloux *et al*., 1982). Furthermore, all volume translation methods were initially developed for pure components. A few were later extended to be applicable to multicomponent systems (Tsai and Chen, 1998; Lin and Duan, 2005; Abudour *et al*., 2013).

1.2. Literature Review

1.2.1. Review on CEOS

1.2.1.1. van der Waals EOS

The famous van der Waals equation of state is shown in Eq. (1) (van der Waals, 1873).

$$P = \frac{RT}{v-b} - \frac{a}{v^2} \tag{1}$$

where P is the system pressure, T is the system temperature, R is the universal gas constant, v is the molar volume, a and b are the parameters representing the attractive intermolecular force and the repulsive intermolecular force, respectively. The expressions of the EOS parameters a and b can be found in Eq. (2).

$$\begin{cases} a = \dfrac{27}{64}\dfrac{R^2T_c^2}{P_c} \\ b = \dfrac{1}{8}\dfrac{RT_c}{P_c} \end{cases} \tag{2}$$

where P_c is the critical pressure and T_c is the critical temperature. The van der Waals equation of state laid the very foundation for the various more sophisticated EOSs developed later.

1.2.1.2. Redlich-Kwong EOS (RK-EOS)

RK-EOS was developed in 1949 (Redlich and Kwong, 1949) based on the van der Waals equation of state. The expression of the RK-EOS is found in Eq. (3).

$$P = \frac{RT}{v-b} - \frac{a}{T_r^{0.5}v(v+b)} \tag{3}$$

where T_r is the reduced temperature. The EOS parameters a and b in the RK-EOS are shown in Eq. (4).

$$\begin{cases} a = 0.42747 \dfrac{R^2 T_c^2}{P_c} \\ b = 0.08664 \dfrac{R T_c}{P_c} \end{cases} \tag{4}$$

RK-EOS replaced the term v^2 in the van der Waals equation of state with $v(v+b)$, resulting in improved phase behavior predictions.

1.2.1.3. Soave-Redlich-Kwong EOS (SRK-EOS)

SRK-EOS (Soave, 1972) follows the basic formula of RK-EOS with the addition of a component-dependent correction term α, which is the so-called alpha function. The expression of SRK-EOS is given in Eq. (5).

$$P = \frac{RT}{v-b} - \frac{a\alpha(T_r)}{v(v+b)} \tag{5}$$

where the alpha function is a function of reduced temperature and is given as $\alpha(T_r) = [1 + m(1 - T_r^{0.5})]^2$, and $m = 0.48 + 1.574\omega - 0.176\omega^2$ (ω is the acentric factor).

1.2.1.4. Peng-Robinson EOS (PR-EOS)

PR-EOS is currently one of the most widely used EOSs (Peng and Robinson, 1976). PR-EOS is given by Eq. (6).

$$P = \frac{RT}{v-b} - \frac{a\alpha(T_r)}{v(v+b) + b(v-b)} \tag{6}$$

Later, Robinson and Peng (1980) modified the m function within the alpha function as follows.

$$\begin{cases} m = 0.37464 + 1.5422\omega - 0.26992\omega^2, \omega \leq 0.49 \\ m = 0.3796 + 1.485\omega - 0.1644\omega^2 + 0.01667\omega^3, \omega > 0.49 \end{cases} \tag{7}$$

In general, PR-EOS gives a better density prediction than SRK-EOS. Another improvement of PR-EOS over the previous EOSs is that the PR-EOS offers a critical compressibility of 0.307 (Peng and Robinson, 1976), which is closer to experimental data for heavier hydrocarbons compared to the critical compressibility yielded by the previous EOS (Lopez-Echeverry *et al*., 2017).

1.2.2. Review on Volume Translation Methods

The concept of volume translation was originally proposed by Martin (1967) in an effort to mitigate the difference between his generalized EOS and the previous ones. Later in 1982, Peneloux *et al.* (1982) applied a simple constant volume correction term to improve the density prediction by SRK-EOS. The authors also mathematically proved that the constant volume translation does not affect the equilibrium prediction for pure components and multicomponent systems calculated by SRK-EOS. However, due to the simplicity of the constant volume correction term, this method performs weakly in correcting the density prediction near the critical point.

Temperature-dependent volume correction functions were developed as a more complex form of volume translation methods to improve the capability of CEOS in predicting phase densities near the critical point. Watson *et al*. (1986) proposed a temperature-dependent volume translation method specifically for van der Waals EOS. Later, Mathias *et al*. (1989) proposed a dimensionless distance function that is related to the inverse of the isothermal compressibility. This dimensionless distance function effectively improves the phase densities prediction near the critical region. At almost the same time, this dimensionless

distance function was also used by Chou and Prausnitz (1989) to introduce a phenomenological correction to SRK EOS. Magoulas and Tassios (1990) developed a volume translation method with a modified alpha function. They suggested that the method they proposed should only be applied to correct the phase density prediction for normal alkanes up to *n*-C_{20}. Ungerer *et al*. (1997) correlated the volume translation parameters in PR-EOS as a function of component molecular weight. This technique was also applied later by De Sant'Ana *et al.* (1999). In 1998, two additional volume translation parameters were introduced by Tsai and Chen (1998) to improve the saturated density prediction of PR-EOS. Pederson *et al*. (2004) developed a volume translation method that can be used for density prediction for paraffins that contain a noticeable amount of C_{81+}. More recently, Baled *et al*. (2012) developed a linear temperature-dependent volume translation method to improve the accuracy of density prediction for pure components at high-temperature and high-pressure conditions. Also in 2012, Abudour *et al*. (2012) developed a volume translation method based on the dimensionless distance function that can be used to improve the density prediction in both the single-phase region and the saturated region. Later in 2013, this method was extended to enable it applicable to multicomponent systems (Abudour *et al*., 2013). A comparative study by Young *et al.* (2017) suggests that the volume translated PR-EOS developed by Abudour *et al*. (2012 and 2013) gives the most accurate saturated-liquid density prediction among the popular volume translation methods examined. In view of its good accuracy, the volume translation method proposed by Abudour *et al*. (2013) is selected to be used in this study.

1.2.3. Phase Behavior in a Confined Space

Study on reservoir fluids phase equilibrium in confined nanopores with the consideration of capillary pressure was first carried out by Brusllovsky (1992). A new equation of state was introduced in this work to reflect the effect of capillary pressure on the calculations of thermodynamic properties of pure components and multicomponent systems. Calculation results show that, at a given temperature, dew point pressure increases from the bulk one, and bubble point pressure decreases from the bulk one due to capillary pressure (Brusllovsky 1992). Multiple pieces of research works were conducted on the same subject afterword, but reported that dew point pressure decreases due to capillary pressure (Al-Rub and Datta, 1999; Hamada *et al*., 2007; Qi *et al.*, 2007; Wang *et al.*, 2013; Sandoval *et al*., 2016; Zhang *et al*., 2017; Li *et al*., 2018). The finding of a dew point pressure reduction due to capillary pressure was also later proved experimentally by Qiu *et al.* (2018) and Zhong *et al.* (2018). They measured the dew point of the methane-ethane (C_1-C_2) mixture and the methane-propane (C_1-C_3) mixture at different temperatures and pore radii. They all observed a significant reduction of the dew point pressure due to large capillary pressure present in a confined space. Nojabaei *et al*. (2013) analyzed the entire two-phase envelope under the effect of large capillary pressure. They concluded that dew point pressure decreases at pressures below the cricondentherm point and increases at pressures above the cricondentherm point. They also stated that capillary pressure becomes zero at the critical point due to the vanishing of the vapor-liquid interfacial tension (IFT). Therefore, a two-phase equilibrium does not deviate from the bulk condition at the critical point (Nojabaei *et al*. 2013). More recently, Rezaveisi *et al*., (2018) proposed a strategy to determine the maximum capillary pressure in a two-

phase system at given temperature and pressure. The maximum capillary pressure of a two-phase system is defined as the capillary pressure above which a two-phase equilibrium becomes impossible. They suggested that this capillary equilibrium limit calculation can be applied to the compositional reservoir simulator to improve computational efficiency of reservoir simulations (Rezaveisi *et al*., 2018).

1.3. Problem Statement

In most of the theoretical works that study multiphase equilibrium in confined nanopores, vapor-liquid IFT is generally calculated using the Parachor model (Weinaug and Katz, 1943), which requires an input of phase densities. However, the liquid-phase density predicted directly by PR-EOS is inaccurate. This leads to incorrect IFT calculation, which in turn results in errorneously predicted multiphase equilibrium in confined nanopores.

1.4. Research Objectives

- To apply the volume translation method (Abudour *et al.*, 2013) in PR-EOS to obtain a more accurate density prediction that can be used for more accurate IFT calculations.
- To conduct vapor-liquid IFT calculations using the phase density corrected by volume translation method, and to validate the IFT calculation results with the experimental data collected from literature.
- To develop a new two-phase flash calculation algorithm coupled with volume translation (Abudour *et al.*, 2013) and capillarity effect in a confined space.

1.5. Thesis Structure

This thesis contains four chapters:

- **Chapter 1** introduces the overall scope of this thesis. Research background, literature review, problem statement, research objectives, and thesis structure are presented in this chapter.
- **Chapter 2** introduces the volume translation method proposed by Abudour *et al* (2013) for multicomponent systems. This method is employed in the IFT calculation for the C_1-C_3 mixture and the calculation results are validated by experimental data. The volume translation method is then coupled with the two-phase equilibrium calculation that considers the capillarity effect, and calculation procedure of the proposed two-phase equilibrium calculation algorithm is also presented.
- **Chapter 3** conducts two-phase equilibrium calculations using the proposed algorithm for two binary hydrocarbon mixtures C_1-C_2 and C_1-C_3 in confined nanopores. The volume translation method proposed by Abudour *et al*. (2013) is applied during the calculation. The calculated results are then compared with experimental data collected from literature. Major findings are discussed in this chapter.
- **Chapter 4** presents conclusions of this study and recommendations for future work in this area.

References

Abu Al-Rub, F., and Datta, R. Theoretical Study of Vapor–Liquid Equilibrium inside Capillary Porous Plates. Fluid Phase Equilibria, 162(1-2), (1999) pp.83-96.

Abudour, A., Mohammad, S., Robinson, R., and Gasem, K. Volume-Translated Peng–Robinson Equation of State for Saturated and Single-Phase Liquid Densities. Fluid Phase Equilibria, 335, (2012) pp.74-87.

Abudour, A., Mohammad, S., Robinson, R., and Gasem, K. Volume-Translated Peng-Robinson Equation of State for Liquid Densities of Diverse Binary Mixtures. Fluid Phase Equilibria, 349, (2013) pp.37-55.

Ahlers, J., Yamaguchi, T., and Gmehling, J. Development of a Universal Group Contribution Equation of State. 5. Prediction of the Solubility of High-Boiling Compounds in Supercritical Gases with the Group Contribution Equation of State Volume-Translated Peng−Robinson. Industrial & Engineering Chemistry Research, 43(20), (2004) pp.6569-6576.

Baled, H., Enick, R., Wu, Y., McHugh, M., Burgess, W., Tapriyal, D., and Morreale, B. Prediction of Hydrocarbon Densities at Extreme Conditions Using Volume-Translated SRK and PR Equations of State fit to High Temperature, High Pressure PVT Data. Fluid Phase Equilibria, 317, (2012) pp.65-76.

Brusilovsky, A. Mathematical Simulation of Phase Behavior of Natural Multicomponent Systems at High Pressures with an Equation of State. SPE Reservoir Engineering, 7(01), (1992) pp.117-122.

Chou, G. and Prausnitz, J. A Phenomenological Correction to an Equation of State for the Critical Region. Aiche Journal, 35(9), (1989) pp.1487-1496.

de Sant'Ana, H., Ungerer, P., and de Hemptinne, J. Evaluation of an Improved Volume Translation for the Prediction of Hydrocarbon Volumetric Properties. Fluid Phase Equilibria, 154(2), (1999) pp.193-204.

Dong, X., Liu, H., Hou, J., Wu, K., and Chen, Z. Phase Equilibria of Confined Fluids in Nanopores of Tight and Shale Rocks Considering the Effect of Capillary Pressure and Adsorption Film. Industrial & Engineering Chemistry Research, 55(3), (2016) pp.798-811.

Hamada, Y., Koga, K., and Tanaka, H. Phase Equilibria and Interfacial Tension of Fluids Confined in Narrow Pores. The Journal of Chemical Physics, 127(8), (2007) 084908.

Li, Y., Kou, J., and Sun, S. Thermodynamically Stable Two-Phase Equilibrium Calculation of Hydrocarbon Mixtures with Capillary Pressure. Industrial & Engineering Chemistry Research, 57(50), (2018) pp.17276-17288.

Lin, H. and Duan, Y. Empirical Correction to the Peng–Robinson Equation of State for the Saturated Region. Fluid Phase Equilibria, 233(2), (2005) pp.194-203.

Lopez-Echeverry, J., Reif-Acherman, S., and Araujo-Lopez, E. Peng-Robinson Equation of State: 40 Years through Cubics. Fluid Phase Equilibria, 447, (2017) pp.39-71.

Magoulas, K. and Tassios, D. Thermophysical Properties of n-Alkanes from C1 to C20 and Their Prediction for Higher Ones. Fluid Phase Equilibria, 56, (1990) pp.119-140.

Martin, J. Equations of State – Applied Thermodynamics Symposium. Industrial & Engineering Chemistry, 59(12), (1967) pp.34-52.

Mathias, P., Naheiri, T., and Oh, E. A Density Correction for the Peng—Robinson Equation of State. Fluid Phase Equilibria, 47(1), (1989) pp.77-87.

Nojabaei, B., Johns, R., and Chu, L. Effect of Capillary Pressure on Phase Behavior in Tight Rocks and Shales. SPE Reservoir Evaluation & Engineering, 16(03), (2013) pp.281-289.

Pedersen, K., Milter, J., and Sørensen, H. Cubic Equations of State Applied to HT/HP and Highly Aromatic Fluids. SPE Journal, 9(02), (2004) pp.186-192.

Péneloux, A., Rauzy, E., and Fréze, R. A Consistent Correction for Redlich-Kwong-Soave Volumes. Fluid Phase Equilibria, 8(1), (1982) pp.7-23.

Peng, D. and Robinson, D. A New Two-Constant Equation of State. Industrial & Engineering Chemistry Fundamentals, 15(1), (1976) pp.59-64.

Qi, Z., Liang, B., Deng, R., Du, Z., Wang, S., and Zhao, W. Phase Behavior Study in the Deep Gas-Condensate Reservoir with Low Permeability. In: SPE Europec/EAGE Annual Conference and Exhibition. London: Society of Petroleum Engineers (2007).

Qiu, X., Tan, S., Dejam, M., and Adidharma, H. Simple and Accurate Isochoric Differential Scanning Calorimetry Measurements: Phase Transitions for Pure Fluids and Mixtures in Nanopores. Physical Chemistry Chemical Physics, 21(1), (2018) pp.224-231.

Redlich, O. and Kwong, J. On the Thermodynamics of Solutions. V. An Equation of State. Fugacities of Gaseous Solutions. Chemical Reviews, 44(1), (1949) pp.233-244.

Rezaveisi, M., Sepehrnoori, K., Pope, G., and Johns, R. Thermodynamic Analysis of Phase Behavior at High Capillary Pressure. SPE Journal, 23(06), (2018) pp.1977-1990.

Robinson, D. and Peng, D. The Characterization of the Heptanes and HeavierFractions for the GPA Peng-Robinson Programs. Research Report (Gas Pro-cessors Association), Gas Processors Association, (1978).

Sandoval, D., Yan, W., Michelsen, M., and Stenby, E. Phase Envelope Calculations for Reservoir Fluids in the Presence of Capillary Pressure. In: SPE Annual Technical Conference and Exhibition. Houston: Society of Petroleum Engineers (2015).

Sandoval, D., Yan, W., Michelsen, M., and Stenby, E. The Phase Envelope of Multicomponent Mixtures in the Presence of a Capillary Pressure Difference. Industrial & Engineering Chemistry Research, 55(22), (2016) pp.6530-6538.

Sandoval, D., Yan, W., Michelsen, M., and Stenby, E. Influence of Adsorption and Capillary Pressure on Phase Equilibria inside Shale Reservoirs. Energy & Fuels, 32(3), (2018) pp.2819-2833.

Shi, J., Li, H., and Pang, W. An Improved Volume Translation Strategy for PR EOS without Crossover Issue. Fluid Phase Equilibria. 470, (2018) pp.164-175.

Soave, G. Equilibrium Constants from a Modified Redlich-Kwong Equation of State. Chemical Engineering Science, 27(6), (1972) pp.1197-1203.

Tsai, J. and Chen, Y. Application of a Volume-Translated Peng-Robinson Equation of State on Vapor-Liquid Equilibrium Calculations. Fluid Phase Equilibria, 145(2), (1998) pp.193-215.

Ungerer, P. and Batut, C. Prédiction des Propriétés Volumétriques des Hydrocarbures par une Translation de Volume Améliorée. Revue de l'Institut Français du Pétrole, 52(6), (1997) pp.609-623.

van der Waals, J.D. Continuity of the Gaseous and Liquid State of Matter (1873).

Wang, Y., Yan, B., and Killough, J. Compositional Modeling of Tight Oil Using Dynamic Nanopore Properties. In: SPE Annual Technical Conference and Exhibition. New Orleans: Society of Petroleum Engineers (2013).

Watson, P., Cascella, M., May, D., Salerno, S., and Tassios, D. Prediction of vapor Pressures and Saturated Molar Volumes with a Simple Cubic Equation of State: Part II: The van der Waals - 711 EOS. Fluid Phase Equilibria, 27, (1986) pp.35-52.

Weinaug, C. and Katz, D. Surface Tensions of Methane-Propane Mixtures. Industrial & Engineering Chemistry, 35(2), (1943) pp.239-246.

Young, A.F., Pessoa, F.L.P., and Ahon, V.R.R. Comparison of Volume Translation and Co-Volume Functions Applied in the Peng-Robinson EOS for Volumetric Corrections. Fluid Phase Equilibria, 435, (2017) pp.73-87.

Zhang, Y., Lashgari, H., Di, Y., and Sepehrnoori, K. Capillary Pressure Effect on Phase Behavior of CO_2/Hydrocarbons in Unconventional Reservoirs. Fuel, 197, (2017) pp.575-582.

Zhong, J., Zhao, Y., Lu, C., Xu, Y., Jin, Z., Mostowfi, F., and Sinton, D. Nanoscale Phase Measurement for the Shale Challenge: Multicomponent Fluids in Multiscale Volumes. Langmuir, 34(34), (2018) pp.9927-9935.

CHAPTER 2 VOLUME TRANSLATION METHOD AND NUMERICAL ALGORITHM OF TWO-PHASE EQUILIBRIUM CALCULATION IN CONFINED NANOPORES

2.1. Volume Translation Method

The constant volume translation method is given by Eq. (8) (Peneloux *et al.*, 1982).

$$V_{corr} = V_{PR} + C \tag{8}$$

where V_{corr} is the corrected molar volume, V_{PR} is the original molar volume calculated by the PR-EOS, and C is the volume translation term. This method was originally proposed to be applied for pure substances and can be extended to mixtures by using a given mixing rule. Abudour *et al.* (2013) extended the volume translation method developed by them (Abudour *et al.*, 2012) to the multicomponent mixtures. The volume translation method developed by Abudour *et al*. (2013) is given in Eq. (9).

$$V_{corr} = V_{PR} + C_m - \delta_m \left(\frac{0.35}{0.35 + d_m} \right) \tag{9}$$

where C_m is the volume translation term from the conventional volume translation method but modified by Abudour *et al*. (2012), δ_m is the volume correction for mixtures, and d_m is the dimensionless distance function. The volume translation term, the volume correction for mixtures, and the dimensionless distance function are three major components in this volume translation method (Abudour *et al.*, 2013). They will be introduced individually in the following sections.

2.1.1. Volume Translation Developed by Abudour *et al.* (2013)

C_m is calculated using Eq. (10) (Abudour *et al*. 2012).

$$C_m = \frac{RT_{cm}}{P_{cm}}[C_{1m} - (0.004 - C_{1m})exp(-2d_m)] \tag{10}$$

where T_{cm} is the critical temperature for mixtures, P_{cm} is the critical pressure for mixtures, and C_{1m} is a fluid-dependent parameter (Peneloux *et al*. 1982). T_{cm} can be calculated using the mixing rule proposed by Chueh and Prausnitz (1967) (See Eq. (11)).

$$T_{cm} = \sum \theta_i T_{ci} \tag{11}$$

where T_{ci} is the critical temperature for the component *i*, and θ_i is the surface fraction of component *i* and can be calculated using Eq. (12) (Chueh and Prausnitz, 1967).

$$\theta_i = \frac{x_i V_{ci}^{\frac{2}{3}}}{\sum x_i V_{ci}^{\frac{2}{3}}} \tag{12}$$

where V_{ci} is the critical molar volume of component *i* and x_i is the molar fraction of component *i* in phase *x*.

P_{cm} is calculated by Eq. (13) (Aalto *et al*., 1995).

$$P_{cm} = \frac{(0.2905 - 0.085\omega_m)RT_{cm}}{V_{cm}} \tag{13}$$

where ω_m is mixture acentric factor. The mixing rule that is used to calculate the mixture acentric factor is given in Eq. (14).

$$\omega_m = \sum x_i \omega_i \tag{14}$$

where x_i is the mole fraction of component *i* in phase *x*, which can be either the vapor phase or the liquid phase.

The mixing rule that is applied to C_{1m} is given in Eq. (15) (Peneloux *et al*., 1982).

$$C_{1m} = \sum x_i C_{1i} \tag{15}$$

and C_{1i} is calculated by Eq. (16) (Abudour *et al.*, 2013).

$$C_{1i} = 0.4266 Z_{exp,i} - 0.1101 \tag{16}$$

where $Z_{exp,i}$ is the experimental critical compressibility factor for component *i*.

2.1.2. Volume Correction Term for Mixtures (δ_m)

δ_m is described in Eq. (17) (Abudour *et al.*, 2013).

$$\delta_{cm} = V_{cm,PR}(x) - V_{cm}(x) \tag{17}$$

where $V_{cm,PR}(x)$ is the predicted mixture critical volume that is calculated from PR-EOS, and $V_{cm}(x)$ is the true mixture critical volume (Abudour *et al*., 2013).

$V_{cm,PR}(x)$ is calculated by Eq. (18).

$$V_{cm,PR}(x) = \frac{RT_{cm}}{P_{cm}}\left(Z_{c,EOS}\right) \tag{18}$$

where $Z_{c,EOS}$ is the calculated critical compressibility factor from the PR-EOS that has a constant value of 0.3074.

$V_{cm}(x)$ is estimated by Eq. (19).

$$V_{cm}(x) = \sum \theta_i V_{ci} \tag{19}$$

2.1.3. Dimensionless Distance Function (d_m)

The dimensionless distance function was originally proposed by Mathias *et al*. (1988) for pure substances and is given in Eq. (20).

$$d = \frac{1}{RT_c}\left(\frac{\partial P_{PR}}{\partial \rho}\right)_T \tag{20}$$

where R is the universal gas constant, T_c is the critical temperature and ρ is the molar density of a mixture. The dimensionless distance function is both temperature-dependent and pressure-dependent. Abudour *et al*. (2013) further extended this dimensionless distance function to make it applicable to multicomponent systems. The dimensionless distance function for a multicomponent system is given in Eq. (21) (Mathias *et al*., 2014).

$$d_m = \frac{1}{RT_{cm}}\left(\frac{\partial P_{PR}}{\partial \rho_m}\right)_T - \left(\frac{1}{RT_{cm}\rho^2}\right)\frac{a_{v1}^2}{a_{11}} \tag{21}$$

where ρ_m is the molar density of a mixture, a_{v1} and a_{11} are two molar Helmholtz energy variables. However, in this study, the Helmholtz energy is neglected (Mathias *et al*., 2014).

2.2. Two-Phase Equilibrium Calculation Algorithm Considering Capillary Pressure

The multiphase equilibrium calculation algorithm developed in this thesis work is composed of two iteration loops: an outer loop and an inner loop. The outer loop checks for the fugacity-equality condition, while the inner loop solves for the Rachford-Rice equation.

2.2.1. Outer Loop

A two-phase equilibrium is reached when the chemical-potential-equality condition is satisfied at given temperature, pressure and mixture composition (Whitson and Brulé, 2000). The chemical-potential-equality condition is given in Eq. (22).

$$\mu_{ix}(P_l, T, z_i) = \mu_{iy}(P_v, T, z_i) \qquad i = 1, \dots, N_c \tag{22}$$

where μ_{ix} and μ_{iy} are the chemical potentials of the *i*th component in the liquid phase and the vapor phase, respectively, P_l is the liquid-phase pressure, P_v is the vapor-phase pressure. Due to the capillarity effect in confined nanopores, the wetting phase (liquid phase) pressure will be smaller than the non-wetting phase (vapor phase) pressure. The chemical-potential-equality condition can be converted to the fugacity-equality condition as per Eq. (23).

$$f_{ix}(P_l, T, z_i) = f_{iy}(P_v, T, z_i) \quad i = 1, \dots, N_c \tag{23}$$

where f_{ix} and f_{iy} are the fugacity of the *i*th component in the liquid phase and the vapor phase, respectively. The outer loop solves for fugacity-equality condition and updates the phase equilibrium ratio (k_i) if the fugacity-equality condition is not satisfied. To calculate the component fugacity f_{ix} and f_{iy}, PR-EOS is applied in this algorithm (Peng and Robinson, 1976). The formula that calculates the component fugacity is given in Eq. (24).

$$ln\frac{f_i}{x_i P} = ln\,\phi_i = \frac{B_i}{B}(Z-1) - ln(Z-B) + \frac{A}{2\sqrt{2}B}\left(\frac{B_i}{B} - \frac{2}{A}\sum_{i=1}^{N_c} y_i A_{ij}\right) ln\left(\frac{Z+\left(1+\sqrt{2}B\right)}{Z-\left(1-\sqrt{2}B\right)}\right)$$

$$i = 1, \dots, N_c \tag{24}$$

where x_i is the mole fraction of the *i*th component in any phase, ϕ_{ix} is the fugacity coefficient, and Z is the compressibility factor. A and B are PR-EOS constants. Given that the vapor-phase pressure and the liquid-phase pressure are different due to capillary pressure, the fugacity of the *i*th component in the liquid phase and vapor phase can be calculated from Eq. (25) and Eq. (26), respectively (Nojabaei *et al*., 2013; Sun and Li, 2019).

$$ln\frac{f_{ix}}{x_i P_l} = ln\,\phi_{ix} = \frac{B_i}{B}(Z-1) - ln(Z-B) + \frac{A}{2\sqrt{2}B}\left(\frac{B_i}{B} - \frac{2}{A}\sum_{i=1}^{N_c} x_i A_{ij}\right) ln\left(\frac{Z+\left(1+\sqrt{2}B\right)}{Z-\left(1-\sqrt{2}B\right)}\right),$$

$$i = 1, \dots, N_c \tag{25}$$

$$ln\frac{f_{iy}}{y_i P_v} = ln\,\phi_{iy} = \frac{B_i}{B}(Z-1) - ln(Z-B) + \frac{A}{2\sqrt{2}B}\left(\frac{B_i}{B} - \frac{2}{A}\sum_{i=1}^{N_c} y_i A_{ij}\right) ln\left(\frac{Z+\left(1+\sqrt{2}B\right)}{Z-\left(1-\sqrt{2}B\right)}\right),$$

$$i = 1, \dots, N_c \tag{26}$$

The vapor-phase pressure and the liquid-phase pressure can be related by Eq. (27).

$$P_c = P_v - P_l \tag{27}$$

where P_c is the capillary pressure of the adjacent phases. To calculate the capillary pressure, the Young-Laplace equation (Young, 1805) is used in this study with assumptions of equal principle curvature radii and zero contact angle. The Young-Laplace equation is given in Eq. (28) (Young, 1805).

$$P_c = \frac{2\sigma}{r_p} \tag{28}$$

where σ represents the interfacial tension (IFT) between the liquid phase and the vapor phase, while r_p is the pore radius. Parachor model (Weinaug and Katz, 1943) is employed here to

calculate the IFT of the two phases. The general expression of the Parachor model is given in Eq. (29) (Weinaug and Katz, 1943).

$$\sigma = [\sum_{i=1}^{N_c} P_{chi}\left(x_i \frac{\rho_l}{M_l} - y_i \frac{\rho_g}{M_g}\right)]^4, \quad i = 1, \dots, N_c \tag{29}$$

where P_{chi} is the Parachor constant of the *i*th component, ρ_l and ρ_g are the liquid-phase density and the vapor-phase density, respectively, M_l and M_g are the molecular weight of the liquid phase and the vapor phase, respectively. In the proposed two-phase equilibrium calculation algorithm, the liquid-phase density and the vapor-phase density are calculated using the volume translation method (Abudour *et al.*, 2013) for a better prediction on phase densities.

2.2.2. Inner Loop

The inner loop solves the Rachford-Rice equation (Rachford and Rice, 1952) using the successive substitution method. The mole fraction of each phase (β_x, β_y) and the phase compositions (x_i, y_i) can be obtained upon the completion of this iteration loop. The Rachford-Rice equation is given in Eq. (30).

$$\sum_{i=1}^{N_c}(y_i - x_i) = \sum_{i=1}^{N_c}\left(\frac{z_i(k_i - 1)}{1 + \beta_y(k_i - 1)}\right) = 0 \quad i = 1, \dots, N_c \tag{30}$$

where β_y is the mole fraction of the vapor phase and k_i is the phase equilibrium ratio which can be initialized by Wilson equation (Wilson 1969) shown in Eq. (31).

$$k_i = \frac{P_{ci}}{P} exp[\,5.37(1 + \omega_i)(1 - \frac{T_{ci}}{T})]$$

$$i = 1, \dots, N_c \tag{31}$$

where P_{ci} is the critical pressure of the *i*th component, T_{ci} is the critical temperature of the *i*th component, ω_i is the acentric factor of the *i*th component, and T is the system temperature.

After the mole fraction of each phase (β_x,β_y) and the phase compositions (x_i, y_i) are obtained, the component fugacity (f_{ix}, f_{iy}) is calculated and checked for the fugacity-equality equation. If the condition is satisfied, the iteration loop is ended and the mole fraction of each phase (β_x, β_y) and the phase compositions (x_i, y_i) can be obtained. If the condition is not satisfied, the phase equilibrium ratio will be updated by the following equation Eq. (32) (Whitson and Brulé, 2000) .

$$k_{iy}^{n+1} = k_{iy}^{n} \frac{f_{iy}^{n}}{f_{ix}^{n}} \quad i = 1, \dots, N_c \tag{32}$$

where *n* represents the current *n*th iteration and *n+1* represents the next iteration. Then the Rachford-Rice equation can be solved by using this updated phase equilibrium ratio to obtain new β_x, β_y and x_i, y_i, until the fugacity-equality condition is satisfied. A flowchart that depicts the procedure of the proposed multiphase equilibrium calculation is given in Fig. 1.

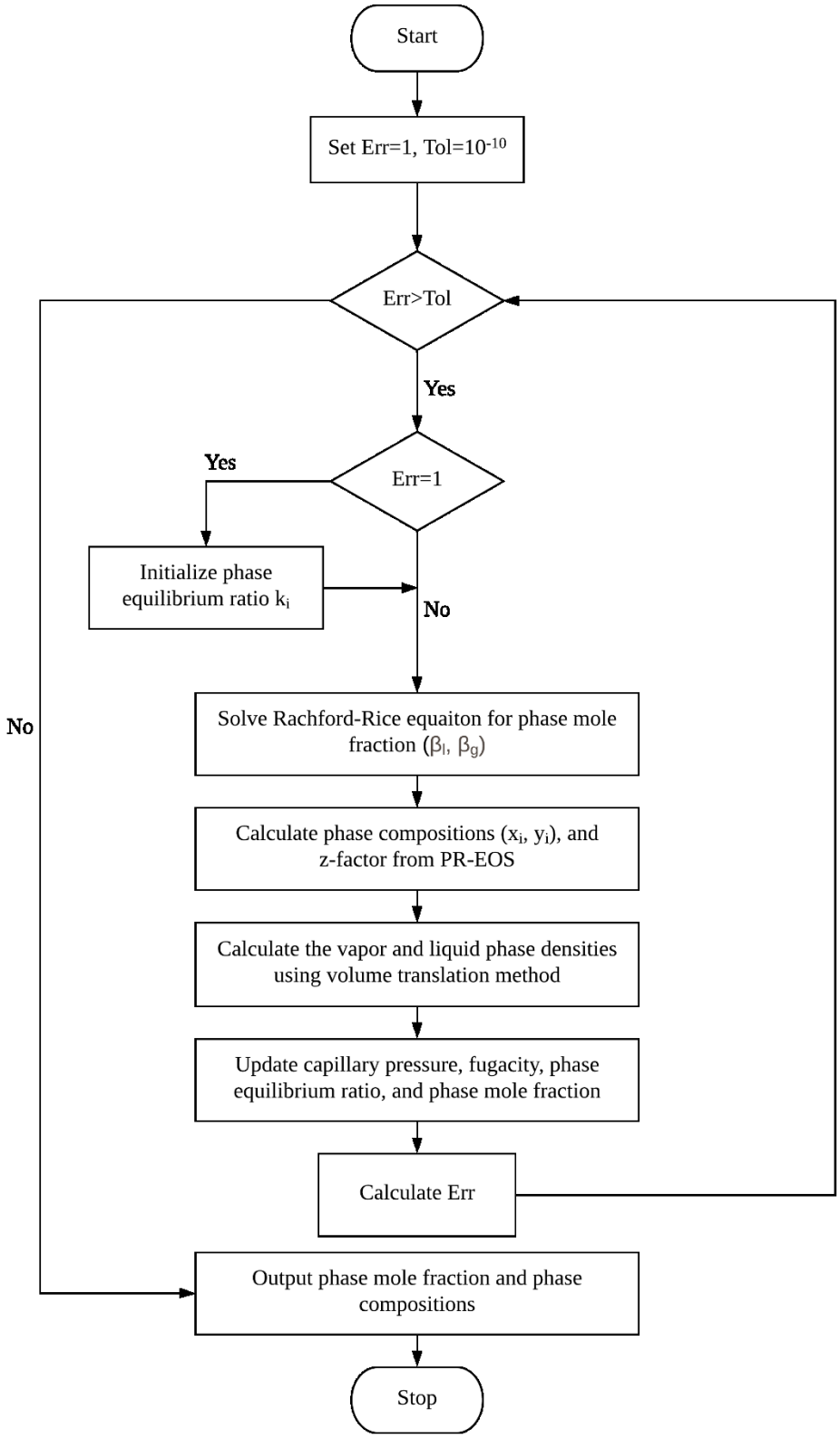

Figure 1: Flowchart of the proposed two-phase equilibrium calculation algorithm coupled with capillary pressure and volume translation (Abudour *et al*., 2013).

2.3. Validation of IFT Calculations

This section presents the IFT calculation results for the binary mixture C_1-C_3 under different temperatures and pressures using the classic Parachor model (Weinaug and Katz, 1943). The effect of applying the volume translation method on hydrocarbon IFT calculation is examined by comparing the IFT calculation results using phase densities predicted directly from the original PR-EOS and phase densities predicted from volume-translated PR-EOS. Experimental IFT data for a C_1-C_3 mixture are collected from the literature (Weinaug and Katz, 1943) to validate the calculation results. A parity plot is presented in Figure 2 to show the effect of applying the volume translation method on the accuracy of IFT calculations.

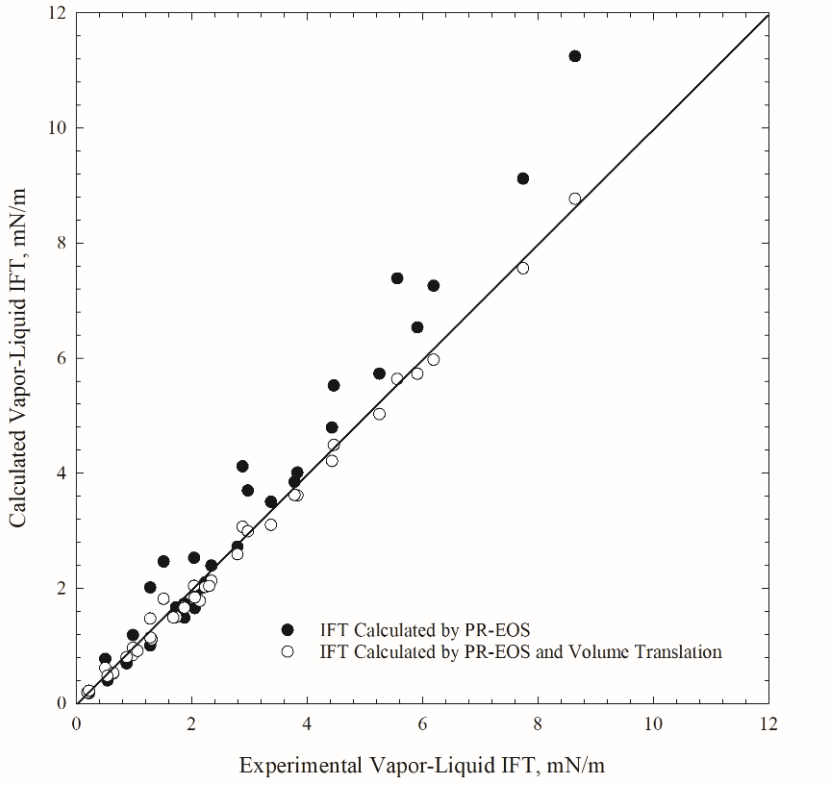

Figure 2: Comparison of calculated vapor-liquid IFT and experimental vapor-liquid IFT for a C_1-C_3 mixture (Weinaug and Katz, 1943).

It is apparent that the IFTs of the mixture C_1-C_3 at different temperatures calculated using the phase densities obtained using volume translation match the experimental data with a much higher accuracy compared to the IFTs calculated directly from PR-EOS. It is proved then that application of the Abudour *et al.* (2013) volume translation method in PR-EOS effectively improves the vapor-liquid IFT prediction for hydrocarbon mixtures.

References

Aalto, M., Keskinen, K., Aittamaa, J. and Liukkonen, S. An Improved Correlation for Compressed Liquid Densities of Hydrocarbons. Part 2. Mixtures. Fluid Phase Equilibria, 114(1-2), (1996) pp.21-35.

Abudour, A., Mohammad, S., Robinson, R., and Gasem, K. Volume-Translated Peng-Robinson Equation of State for Liquid Densities of Diverse Binary Mixtures. Fluid Phase Equilibria, 349, (2013) pp.37-55.

Chueh, P. and Prausnitz, J. Vapor-liquid Equilibria at High Pressures: Calculation of Critical Temperatures, Volumes, and Pressures of Nonpolar Mixtures. AIChE Journal, 13(6), (1967) pp.1107-1113.

Mathias, P., Naheiri, T., and Oh, E. A Density Correction for the Peng—Robinson Equation of State. Fluid Phase Equilibria, 47(1), (1989) pp.77-87.

Nojabaei, B., Johns, R., and Chu, L. Effect of Capillary Pressure on Phase Behavior in Tight Rocks and Shales. SPE Reservoir Evaluation & Engineering, 16(03), (2013) pp.281-289.

Péneloux, A., Rauzy, E., and Fréze, R. A Consistent Correction for Redlich-Kwong-Soave volumes. Fluid Phase Equilibria, 8(1), (1982) pp.7-23.

Peng, D. and Robinson, D. A New Two-Constant Equation of State. Industrial & Engineering Chemistry Fundamentals, 15(1), (1976) pp.59-64.

Rachford, H. and Rice, J. Procedure for Use of Electronic Digital Computers in Calculating Flash Vaporization Hydrocarbon Equilibrium. Journal of Petroleum Technology, 4(10), (1952) pp.19-3.

Sun, H. and Li, H. A New Three-Phase Flash Algorithm Considering Capillary Pressure in a Confined Space. Chemical Engineering Science. 193, (2019) pp.346-363.

Weinaug, C. and Katz, D. Surface Tensions of Methane-Propane Mixtures. Industrial & Engineering Chemistry, 35(2), (1943) pp.239-246.

Whitson, C. and Brulé, M. Phase Behavior. Richardson, TX: Henry L. Doherty Memorial Fund of AIME, Society of Petroleum Engineers (2000).

Wilson, G.M., A Modified Redlich-Kwong Equation of State, Application to General Physical Data Calculations. In: 65th National AIChE Meeting. Cleveland (1969).

Young, T. An Essay on the Cohesion of Fluids. Philosophical Transactions of the Royal Society of London, 95, (1805) pp.65-87.

CHAPTER 3 RESULTS AND DISCUSSION

The proposed two-phase equilibrium calculation algorithm is examined by performing the two-phase equilibrium calculations for two mixtures: C_1-C_2 and C_1-C_3 in a confined space. The feed composition of the mixture C_1-C_2 is 15 mol% of C_1 and 85 mol% of C_3. The feed composition of the mixture C_1-C_3 is 20 mol% of C_1 and 80 mol% of C_3. The properties of the components C_1, C_2, and C_3 involved in the calculations, including critical temperature, critical pressure, acentric factor, critical compressibility, and critical volume, can be found in Table 1.

Table 1: Properties of C_1, C_2, and C_3 (Firoozabadi *et al.*, 1988).

Substances	T_c, K	P_c, bar	ω	Z_c	V_c, cm^3
C_1	190.6	46	0.008	0.2876	99
C_2	305.4	48.84	0.098	0.2789	148
C_3	369.8	42.46	0.152	0.2763	203

The binary interaction parameters (BIPs) used in the PR-EOS model are listed in Table 2 (C_1-C_2) and Table 3 (C_1-C_3).

Table 2: BIP used in PR-EOS model for the mixture C_1-C_2 (Oellrich *et al.*, 1981).

BIPs	C_1	C_2
C_1	0	0.0027
C_2	0.0027	0

Table 3: BIP used in PR-EOS model for the mixture C_1-C_3 (Oellrich *et al.*, 1981).

BIPs	C_1	C_3
C_1	0	0.006
C_2	0.006	0

For each mixture, the two-phase equilibrium is calculated by the two-phase equilibrium calculation coupled with the effect of capillary pressure and the volume translation method

(Abudour *et al.*, 2013). The calculation results are compared with experimental data collected from the literature. Then, the entire two-phase envelope for each mixture is presented to illustrate the effect of volume translation on the two-phase equilibrium calculations in confined nanopores. Finally, a modified Young-Laplace equation (Tan and Piri, 2015) is applied in the algorithm to further improve the accuracy of the proposed two-phase equilibrium calculation algorithm. A general correlation of the tuning parameter lambda (λ) is developed for each mixture. The two-phase equilibrium calculation results using the modified Young-Laplace equation are then validated by experimental data.

3.1. Effect of Volume Translation on Two-Phase Equilibrium Calculations in Confined Nanopores

The effect of applying volume translation in a two-phase equilibrium calculation coupled with capillary pressure is studied in this section. The two-phase equilibrium in confined nanopores for two mixtures C_1-C_2 and C_1-C_3 are calculated using the phase densities predicted from the original PR-EOS and from the volume translation (VT) method (Abudour *et al.*, 2013). The two-phase equilibrium calculations are conducted with three pore radii for the mixture C_1-C_2 and with two pore radii for the mixture C_1-C_3. The calculation results are then summarized and compared with experimental data (Qiu *et al.*, 2018; Zhong *et al.*, 2018). The experimental dew point pressures of the mixture C_1-C_2 and the mixture C_1-C_3 in confined nanopores are collected from Qiu *et al.* (2018) and Zhong *et al*. (2018), respectively. Figures 3-5 show comparisons between calculated and measured dew points in confined nanopores

for the mixture C_1-C_2 with three pore radii. Comparisons between calculated and measured experimental dew points in confined nanopores for the mixture C_1-C_3 with two pore radii are illustrated in Figure 6 and Figure 7.

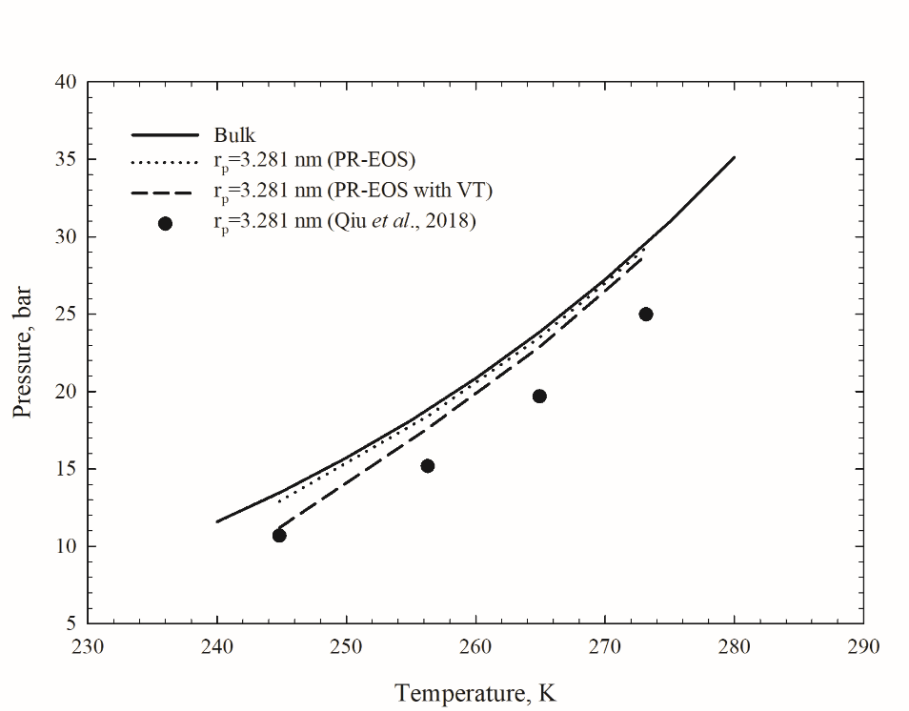

Figure 3: Comparison of measured dew point pressures of the mixture C_1-C_2 in a 3.281 nm nanopore (Qiu *et al.*, 2018) and calculated ones.

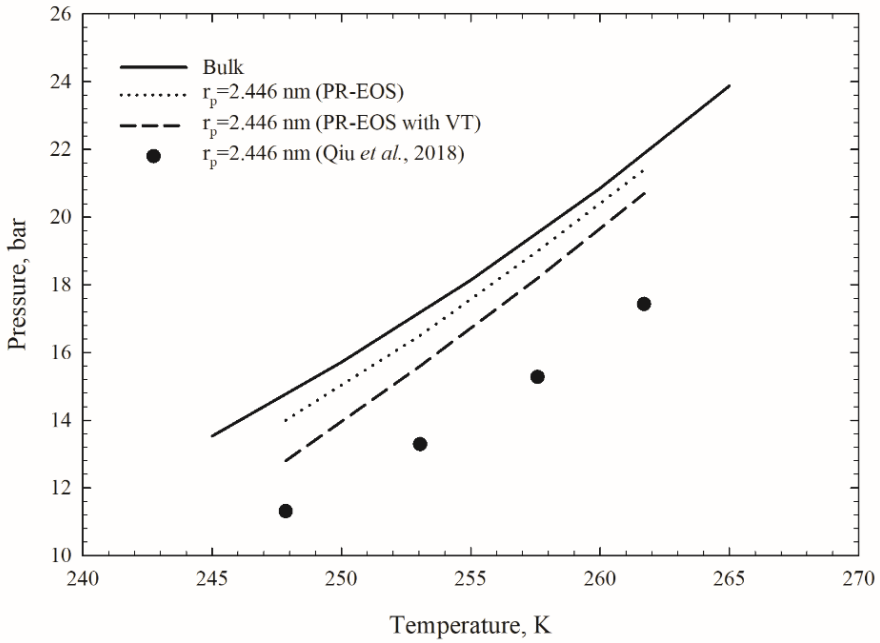

Figure 4: Comparison of measured dew point pressures of the mixture C_1-C_2 in a 2.446 nm nanopore (Qiu *et al*., 2018) and calculated ones.

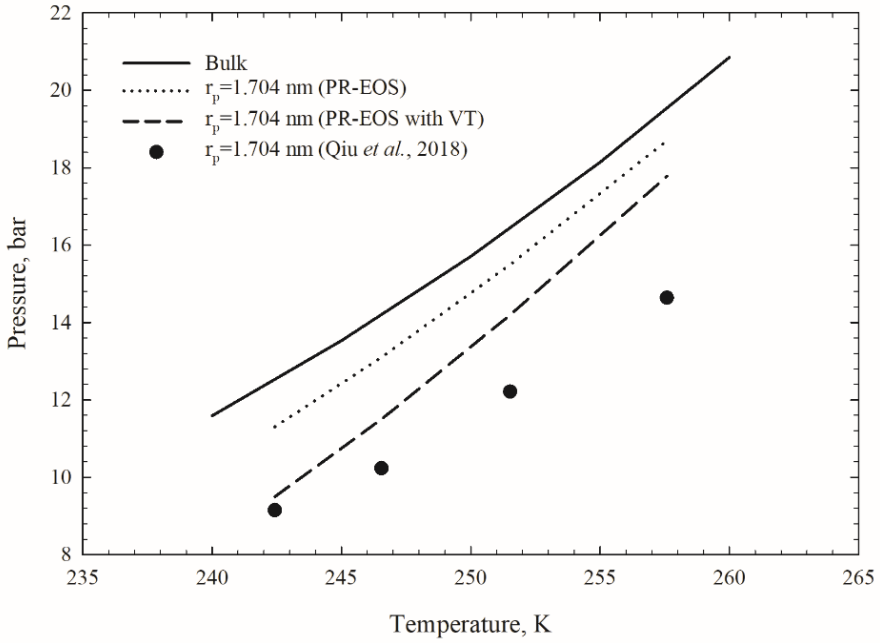

Figure 5: Comparison of measured dew point pressures of the mixture C_1-C_2 in a 1.704 nm nanopore (Qiu *et al*., 2018) and calculated ones.

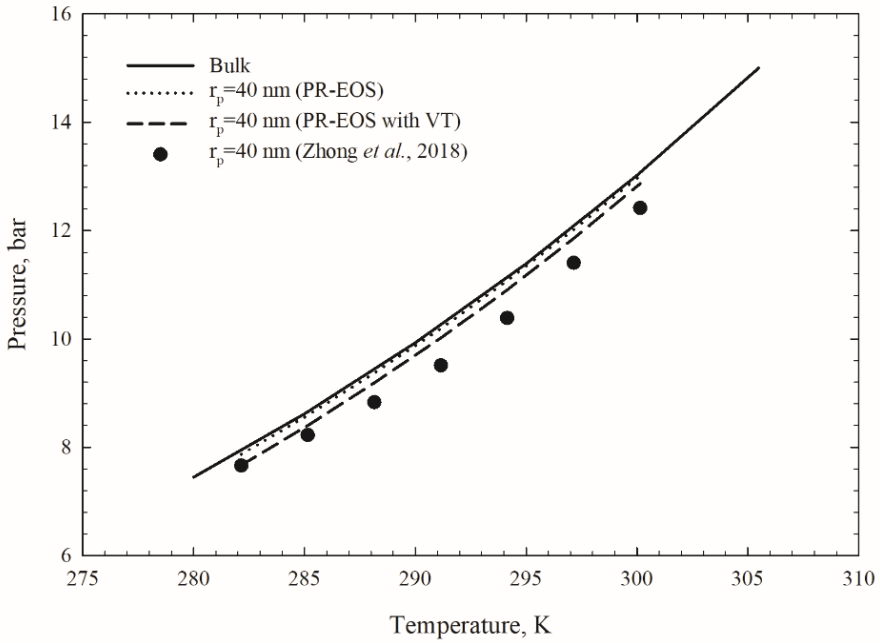

Figure 6: Comparison of measured dew point pressures of the mixture C_1-C_3 in a 40 nm nanopore (Zhong *et al*., 2018) and calculated ones.

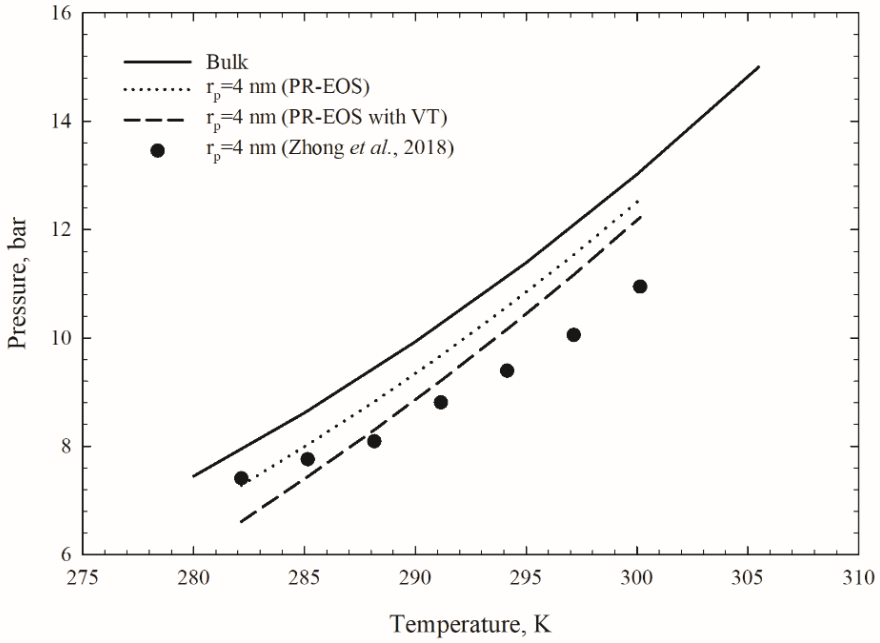

Figure 7: Comparison of measured dew point pressures of the mixture C_1-C_3 a 4 nm nanopore (Zhong *et al*., 2018) and calculated ones.

In the above figures, the solid lines represent the calculated dew point pressures of the tested hydrocarbon mixtures under bulk condition. The dotted lines are the dew point pressures in confined nanopores calculated with the original PR-EOS. The dashed lines are the dew point pressures in confined nanopores calculated with the volume translated PR-EOS (Abudour *et al*., 2013). The circle symbols are the experimental dew point data collected from the literature (Qiu *et al.*, 2018; Zhong *et al.*, 2018). It can be seen from the figures that the dew point pressures for both mixtures in confined nanopore calculated with or without volume translation are all reduced from its bulk condition at a given temperature. This is consistent with the measured dew point pressures in nanopores. However, the dew point pressures calculated by two-phase equilibrium calculations coupled with the volume translation method are much closer to the experimental data compared to those calculated without employing the volume translation method. Application of the volume translation method effectively improves the liquid-phase density prediction for both hydrocarbon mixtures, which in turn provides more accurate IFT calculation results. As such, a more accurate capillary-pressure prediction ensues. Dew point pressures calculated by the two-phase equilibrium calculation with the adjusted capillary pressure thereby show a better match to the measured experimental dew point pressures. It is proved that the application of the volume translation method is effective in improving the accuracy of the two-phase equilibrium calculations in confined nanopores. After the proposed two-phase equilibrium calculation algorithm is validated by experimental data, the entire two-phase envelopes, including the bubble point boundary and the dew point boundary, are calculated with various pore radii for both mixtures. Figures 8-10 show the calculated two-phase envelopes of the mixture C_1-C_2 with

three different pore radii. Figure 11 and Figure 12 show the calculated two-phase envelopes of the mixture C_1-C_3 with two different pore radii.

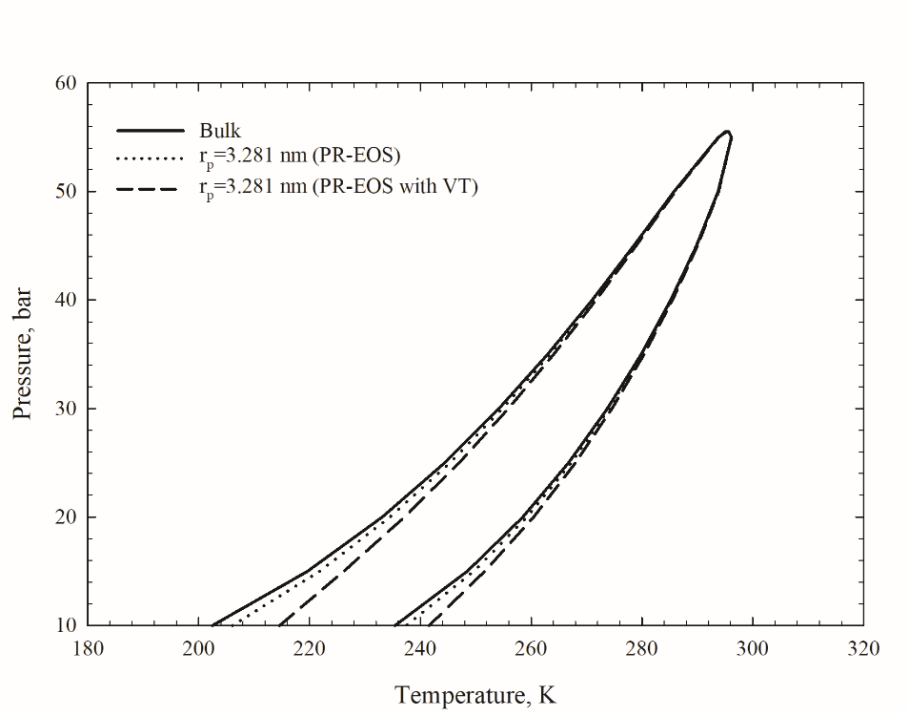

Figure 8: Two-phase envelopes of the mixture C_1-C_2 in a 3.281 nm nanopore calculated by volume translated PR-EOS (Abudour *et al*., 2013).

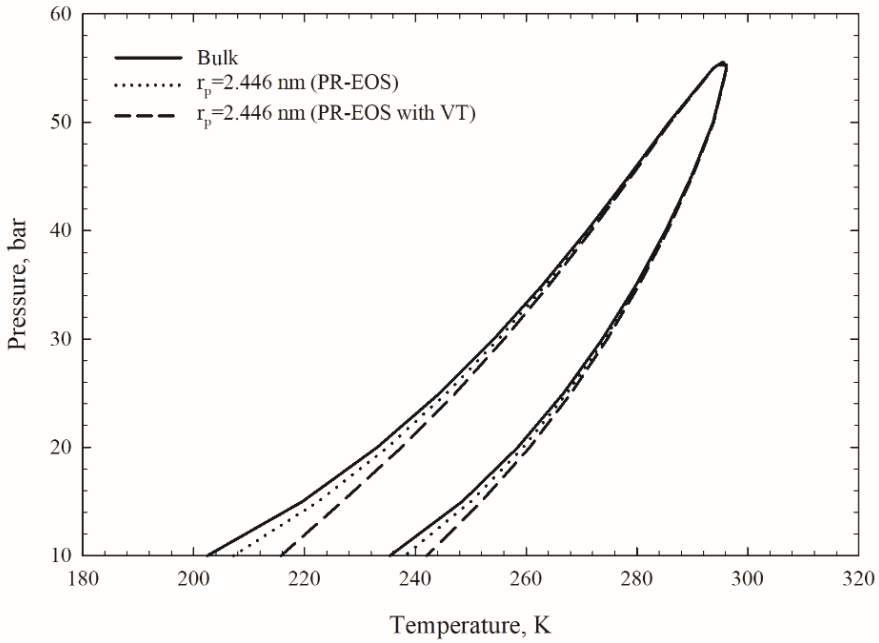

Figure 9: Two-phase envelopes of the mixture *C1-C2* in a 2.446 nm nanopore calculated by volume translated PR-EOS (Abudour *et al*., 2013).

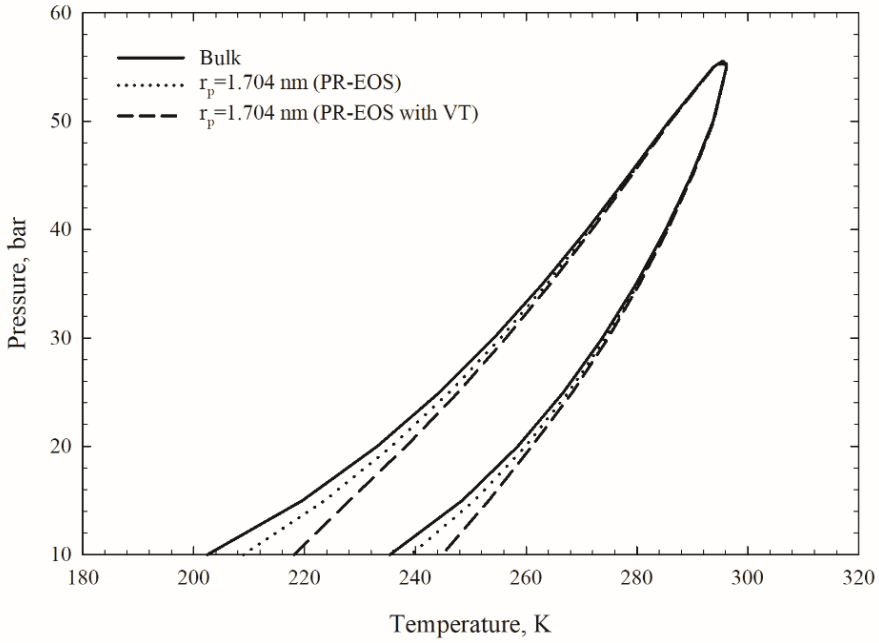

Figure 10: Two-phase envelopes of the mixture *C1-C2* in a 1.704 nm nanopore calculated by volume translated PR-EOS (Abudour *et al*., 2013).

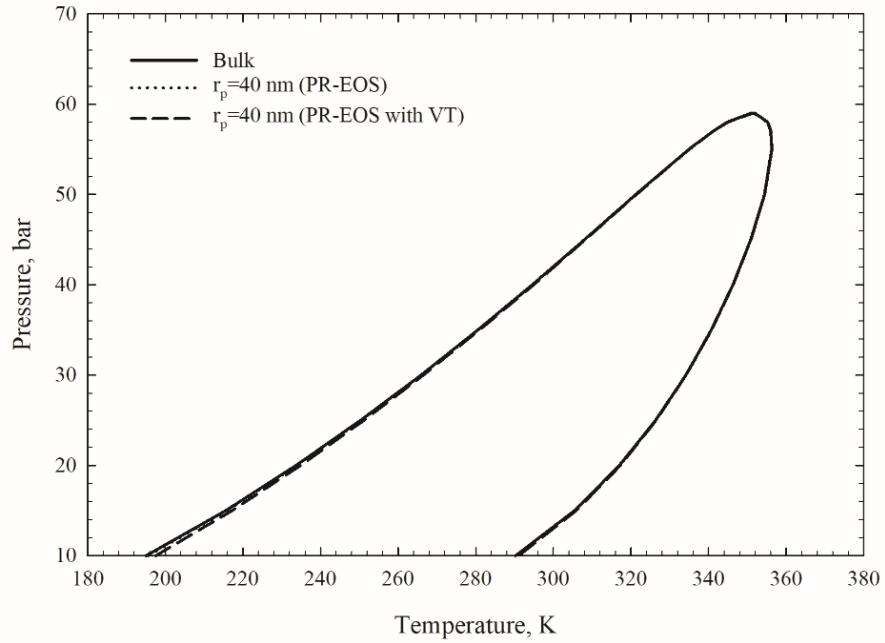

Figure 11: Two-phase envelopes of the mixture C_1-C_3 in a 40 nm nanopore calculated by volume translated PR-EOS (Abudour *et al*., 2013).

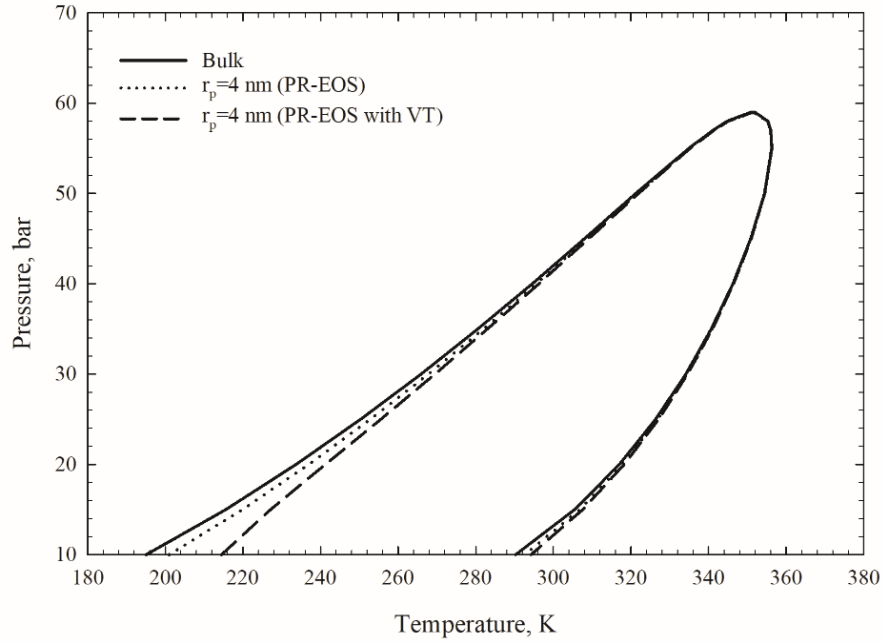

Figure 12: Two-phase envelopes of the mixture C_1-C_3 in a 4 nm nanopore calculated by volume translated PR-EOS (Abudour *et al*., 2013).

It is seen from the above figures that, for both mixtures, the calculated phase boundary in confined nanopores shifts from its bulk ones to higher temperatures at given pressures due to capillary effect. The deviation becomes more obvious with a smaller pore radius. This finding applies to both bubble point boundary and dew point boundary. Implementation of the volume translation method further shifts the phase boundary to the lower right part of the diagram. Given that the proposed two-phase equilibrium calculation algorithm has been previously validated by experimental data, it is concluded that the two-phase envelope calculation is more accurate when the volume translation technique is applied in the PR-EOS model.

3.2. Application of a Modified Young-Laplace Equation in the Proposed Algorithm

Although the application of the volume translation method greatly improves the accuracy of two-phase equilibrium calculations in confined nanopores, the modelling results still do not match very well with the experimental data. To address this issue, this work applies a modified Young-Laplace equation (Tan and Piri, 2015) instead of the original Young-Laplace equation with the assumptions of zero contact angle and equal principle pore radii. Those assumptions made during the calculation weaken the accuracy of the capillary pressure prediction in nanopores. The modified Young-Laplace equation adjusts the calculated capillary pressure by introducing a tuning parameter lambda (λ). A general correlation of the tuning parameter λ for two mixtures C_1-C_2 and C_1-C_3 can be developed by fitting the calculated dew points with the experimental data. The modified Young-Laplace (Tan and Piri, 2015) is given in Eq. (33).

$$P_c = \frac{2\sigma}{r_p(1-\lambda)} \quad (33)$$

The tuning parameter λ is always less than one but can be a negative value. When the λ is between zero and one, the calculated capillary pressure is adjusted to a larger value. When the λ is less than zero, the calculated capillary pressure is adjusted to a lower value. In order to apply the modified Young-Laplace equation in the proposed two-phase equilibrium calculation algorithm, a general correlation of the tuning parameter λ for each mixture needs to be developed. It was previously suggested that the tuning parameter λ is a function of temperature and pore radius (Tan and Piri, 2015), which is proved to be also valid by this study. As for a mixture residing in a given nanopore at a given temperature, the tuning parameter λ is determined by fitting the measured dew point pressure at a given temperature. During the fitting process, firstly a guessed λ value is fed into the two-phase flash calculation algorithm to yield a dew point pressure. λ is tuned until the calculated dew point pressure matches the measured one. The computed tuning parameter λ for the mixtures C_1-C_2 and C_1-C_3 at different temperatures and pore radii is given in Figfure 13 and Figure 14, respectively. Based on the results shown in Figure 13, the following empirical correlation for λ can be obtained for the mixture C_1-C_2 (R^2=0.9992).

$$\lambda = -14.7 + 0.09466T + 0.3595r_p - 0.0001422T^2 - 0.001104Tr_p \quad \#(34)$$

Based on results shown in Figure 14, the following empirical correlation for λ can be developed for the mixture C_1-C_3 (R^2=0.9218).

$$\lambda = -51.85 + 0.2994T + 0.1979r_p - 0.0004148T^2 - 0.0006433Tr_p \quad \#(35)$$

One can observe that the λ correlations for both mixtures show a quadratic polynomial relationship with temperature. Furthermore, λ decreases with a decreasing pore radius.

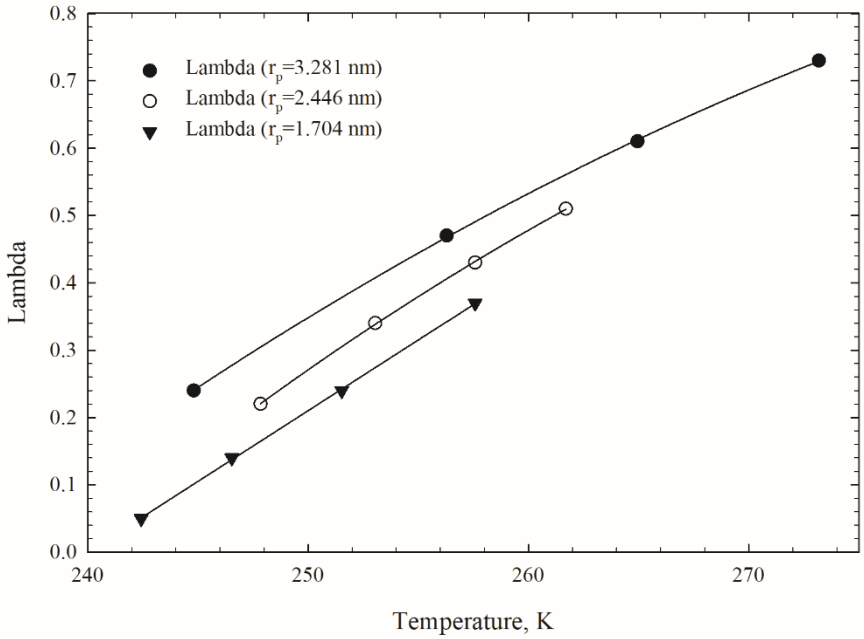

Figure 13: Computed tuning parameter λ for the mixture C_1-C_2 based on the experimental data provided by Qiu *et al*. (2018). The solid lines are trend lines which are drawn for visual guide purpose.

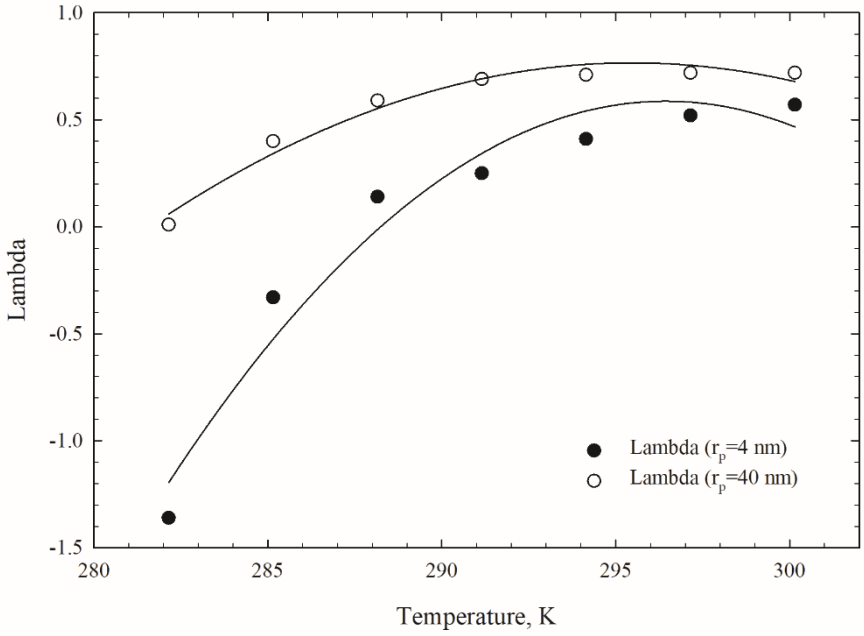

Figure 14: Computed tuning parameter λ for the mixture C_1-C_3 based on the experimental data provided by Zhong *et al*. (2018). The solid lines are trend lines which are drawn for visual guide purpose.

The above correlations of λ for the two mixtures C_1-C_2 and C_1-C_3 can then be implemented in the modified Young-Laplace equation in the proposed algorithm to obtain more accurate two-phase equilibrium calculations in confined nanopores. In addition to the measured dew point pressures, Figure 15 and Figure 16 show the dew point pressure curves of the mixtures C_1-C_2 and C_1-C_3 calculated using the two-phase equilibrium calculation algorithm coupled with both the volume translation (Abudour *et al*., 2013) and the modified Young-Laplace equation (Tan and Piri, 2015).

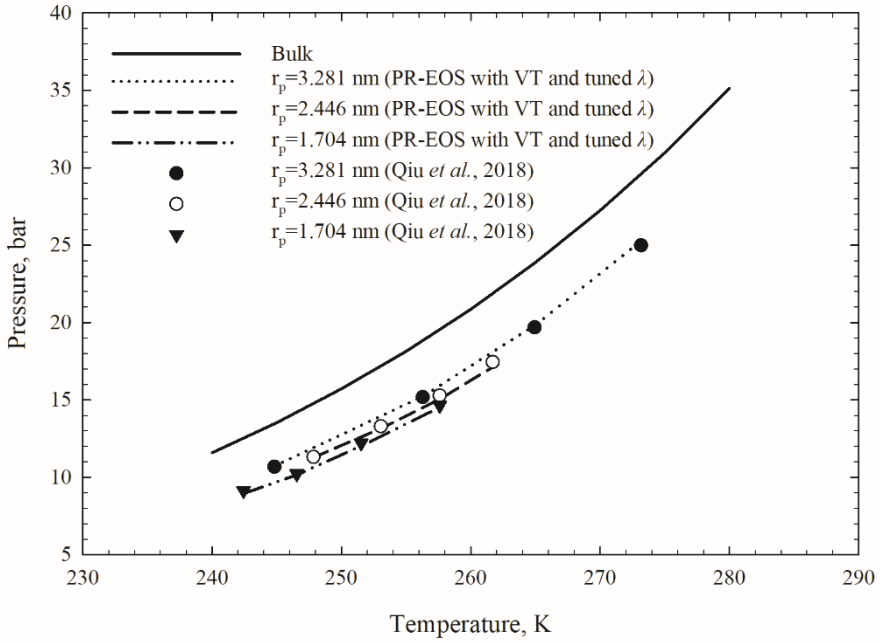

Figure 15: Comparison of measured dew point pressures of the mixture C_1-C_2 (Qiu *et al*., 2018) and calculated ones by the two-phase equilibrium calculation algorithm coupled with the volume translation (Abudour *et al*., 2013) and the modified Young-Laplace equation (Tan and Piri, 2015).

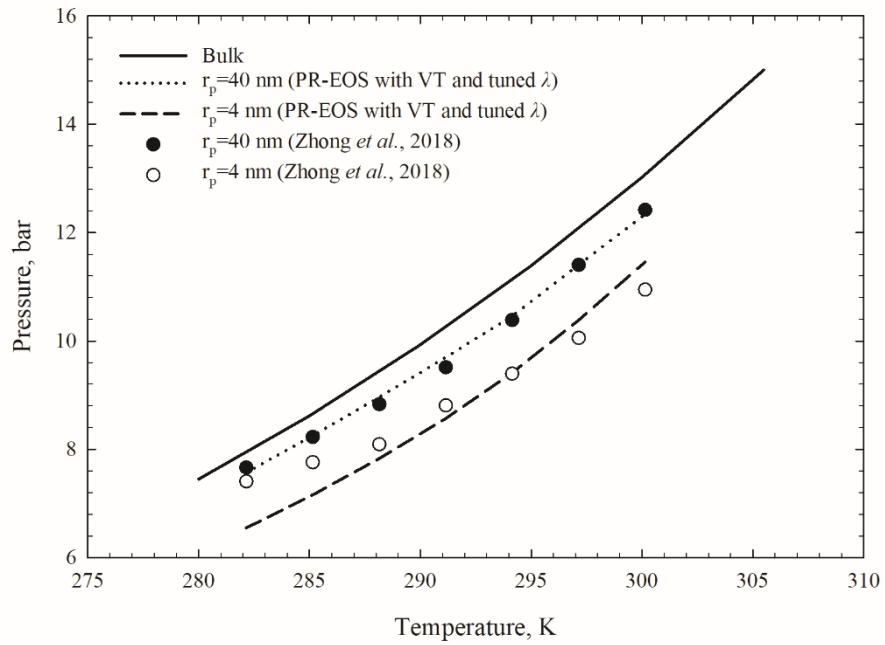

Figure 16: Comparison of measured dew point pressures of the mixture C_1-C_3 (Zhong *et al*., 2018) and calculated ones by the two-phase equilibrium calculation algorithm coupled with the volume translation (Abudour *et al*., 2013) and the modified Young-Laplace equation (Tan and Piri, 2015).

The dew point pressures of the mixtures C_1-C_2 and C_1-C_3 in confined nanopores calculated using the new strategy match the experimental data with a decent accuracy. The modelling of the tuning parameter λ for both tested mixtures is proved to be effective in improving the accuracy of the two-phase equilibrium calculations in confined nanopores.

3.3. Conclusions

The following conclusions can be obtained based on the results presented in this chapter:

1. The dew point pressures of two mixtures C_1-C_2 and C_1-C_3 in confined nanopores calculated by the proposed two-phase equilibrium calculation algorithm with the use of the volume translation method proposed by Abudour *et al.* (2013) are closer to the

experimental data compared with the dew point pressures calculated by the two-phase equilibrium calculation algorithm without the use of the volume translation method proposed by Abudour *et al.* (2013).

2. Two empirical correlations of the tuning parameter λ in the modified Young-Laplace equation are obtained for the two mixtures C_1-C_2 and C_1-C_3 examined in this study. They are shown to be a function of both temperature and nanopore radius.
3. Implementation of the modified Young-Laplace equation in the proposed algorithm can effectively improve the accuracy of the confined dew point predictions for the two hydrocarbon mixtures examined in this study.

References

Abudour, A., Mohammad, S., Robinson, R., and Gasem, K. Volume-Translated Peng-Robinson Equation of State for Liquid Densities of Diverse Binary Mixtures. Fluid Phase Equilibria, 349, (2013) pp.37-55.

Firoozabadi, A. and Katz, D. Surface Tension of Reservoir Crude Oil/Gas Systems Recognizing the Asphalt in the Heavy Fraction. SPE Reservoir Engineering, 3(01), (1988) pp.265-272.

Oellrich, L., Plocker, U., Prausnitz, J., and Knapp, H. Equation-of-State Methods for Computing Phase Equilibria and Enthalpies. Int. Chem. Eng., 21(1), (1981) pp. 1-15.

Qiu, X., Tan, S., Dejam, M., and Adidharma, H. Simple and accurate isochoric differential scanning calorimetry measurements: phase transitions for pure fluids and mixtures in nanopores. Physical Chemistry Chemical Physics, 21(1), (2018) pp.224-231.

Tan, S. and Piri, M. Equation-of-State Modeling of Associating-Fluids Phase Equilibria in Nanopores. Fluid Phase Equilibria, 405, (2015) pp.157-166.

Zhong, J., Zhao, Y., Lu, C., Xu, Y., Jin, Z., Mostowfi, F., and Sinton, D. Nanoscale Phase Measurement for the Shale Challenge: Multicomponent Fluids in Multiscale Volumes. Langmuir, 34(34), (2018) pp.9927-9935.

CHAPTER 4 CONCLUSIONS AND RECOMMENDATIONS

4.1. Conclusions

This work proposes a new two-phase equilibrium calculation algorithm that couples the effect of capillary pressure and volume translation in the conventional two-phase equilibrium calculation algorithm. The volume translation method used to calculate the phase densities in the proposed algorithm was proposed by Abudour *et al*. (2013). This work first studies the effect of volume translation on vapor-liquid IFT calculations and then validates the calculated IFTs with experimental data (Weinaug and Katz, 1943). It is found that by using the phase densities calculated from volume translated PR-EOS, the calculated vapor-liquid IFTs are closer to the experimental data compared to the IFTs calculated using the phase densities from the original PR-EOS. Then, the proposed two-phase equilibrium calculation algorithm is employed to calculate dew point pressures in confined spaces for two hydrocarbon mixtures C_1-C_2 and C_1-C_3. The calculated dew point pressures for both tested mixtures using the proposed algorithm match the experimental data (Qiu *et al.*, 2018; Zhong *et al.*, 2018) with a higher accuracy compared to the dew point pressures calculated without applying the volume translation method. Overall, the application of the volume translation method (Abudour *et al*., 2013) significantly improves the accuracy of the two-phase equilibrium calculations in confined nanopores. Finally, a modified Young-Laplace equation (Tan and Piri, 2015) is used to adjust the prediction of the capillary pressure. Empirical correlations of the tuning parameter λ are developed in this work and applied during the two-phase equilibrium calculations. It is found that the application of the modified Young-Laplace

equation in the proposed two-phase equilibrium calculation algorithm significantly improves the calculation accuracy and the calculated results match very well with the experimental data.

4.2. Recommendations

One limitation of the current work is that limited experimental data are used to validate the proposed modelling methodology. The experimental dew point pressures are only collected for two light hydrocarbon mixtures. The performance of the proposed algorithm on predicting two-phase equilibrium for heavier hydrocarbon mixtures in confined nanopores is uncertain. With more experimental data made available in the future, the proposed algorithm can then be examined on heavy hydrocarbon mixtures. Furthermore, the proposed algorithm only considers capillary pressure in confined nanopores. Other factors (such as adsorption) are not considered. In addition, the shift of critical point in nanopores could be included in the proposed algorithm for a better description of the confinement effect on phase behavior.

References

Abudour, A., Mohammad, S., Robinson, R., and Gasem, K. Volume-Translated Peng-Robinson Equation of State for Liquid Densities of Diverse Binary Mixtures. Fluid Phase Equilibria, 349, (2013) pp.37-55.

Qiu, X., Tan, S., Dejam, M., and Adidharma, H. Simple and accurate isochoric differential scanning calorimetry measurements: phase transitions for pure fluids and mixtures in nanopores. Physical Chemistry Chemical Physics, 21(1), (2018) pp.224-231.

Tan, S. and Piri, M. Equation-of-State Modeling of Associating-Fluids Phase Equilibria in Nanopores. Fluid Phase Equilibria, 405, (2015) pp.157-166.

Weinaug, C. and Katz, D. Surface Tensions of Methane-Propane Mixtures. Industrial & Engineering Chemistry, 35(2), (1943) pp.239-246.

Zhong, J., Zhao, Y., Lu, C., Xu, Y., Jin, Z., Mostowfi, F., and Sinton, D. Nanoscale Phase Measurement for the Shale Challenge: Multicomponent Fluids in Multiscale Volumes. Langmuir, 34(34), (2018) pp.9927-9935.

BIBLIOGRAPHY

Aalto, M., Keskinen, K., Aittamaa, J., and Liukkonen, S. An Improved Correlation for Compressed Liquid Densities of Hydrocarbons. Part 2. Mixtures. Fluid Phase Equilibria, 114(1-2), (1996) pp.21-35.

Abu Al-Rub, F. and Datta, R. Theoretical Study of Vapor–Liquid Equilibrium inside Capillary Porous Plates. Fluid Phase Equilibria, 162(1-2), (1999) pp.83-96.

Abudour, A., Mohammad, S., Robinson, R., and Gasem, K. Volume-Translated Peng–Robinson Equation of State for Saturated and Single-Phase Liquid Densities. Fluid Phase Equilibria, 335, (2012) pp.74-87.

Abudour, A., Mohammad, S., Robinson, R., and Gasem, K. Volume-Translated Peng-Robinson Equation of State for Liquid Densities of Diverse Binary Mixtures. Fluid Phase Equilibria, 349, (2013) pp.37-55.

Ahlers, J., Yamaguchi, T., and Gmehling, J. Development of a Universal Group Contribution Equation of State. 5. Prediction of the Solubility of High-Boiling Compounds in Supercritical Gases with the Group Contribution Equation of State Volume-Translated Peng−Robinson. Industrial & Engineering Chemistry Research, 43(20), (2004) pp.6569-6576.

Baled, H., Enick, R., Wu, Y., McHugh, M., Burgess, W., Tapriyal, D., and Morreale, B. Prediction of Hydrocarbon Densities at Extreme Conditions Using Volume-Translated SRK and PR Equations of State fit to High Temperature, High Pressure PVT Data. Fluid Phase Equilibria, 317, (2012) pp.65-76.

Brusilovsky, A. Mathematical Simulation of Phase Behavior of Natural Multicomponent Systems at High Pressures with an Equation of State. SPE Reservoir Engineering, 7(01), (1992) pp.117-122.

Chou, G. and Prausnitz, J. A Phenomenological Correction to an Equation of State for the Critical Region. AIChE Journal, 35(9), (1989) pp.1487-1496.

Chueh, P. and Prausnitz, J. Vapor-liquid Equilibria at High Pressures: Calculation of Critical Temperatures, Volumes, and Pressures of Nonpolar Mixtures. AIChE Journal, 13(6), (1967) pp.1107-1113.

de Sant'Ana, H., Ungerer, P., and de Hemptinne, J. Evaluation of an Improved Volume Translation for the Prediction of Hydrocarbon Volumetric Properties. Fluid Phase Equilibria, 154(2), (1999) pp.193-204.

Dong, X., Liu, H., Hou, J., Wu, K., and Chen, Z. Phase Equilibria of Confined Fluids in Nanopores of Tight and Shale Rocks Considering the Effect of Capillary Pressure and Adsorption Film. Industrial & Engineering Chemistry Research, 55(3), (2016) pp.798-811.

Firoozabadi, A. and Katz, D. Surface Tension of Reservoir Crude Oil/Gas Systems Recognizing the Asphalt in the Heavy Fraction. SPE Reservoir Engineering, 3(01), (1988) pp.265-272.

Hamada, Y., Koga, K., and Tanaka, H. Phase Equilibria and Interfacial Tension of Fluids Confined in Narrow Pores. The Journal of Chemical Physics, 127(8), (2007) 084908.

Li, Y., Kou, J., and Sun, S. Thermodynamically Stable Two-Phase Equilibrium Calculation of Hydrocarbon Mixtures with Capillary Pressure. Industrial & Engineering Chemistry Research, 57(50), (2018) pp.17276-17288.

Lin, H. and Duan, Y. Empirical Correction to the Peng–Robinson Equation of State for the Saturated Region. Fluid Phase Equilibria, 233(2), (2005) pp.194-203.

Lopez-Echeverry, J., Reif-Acherman, S., and Araujo-Lopez, E. Peng-Robinson Equation of State: 40 Years through Cubics. Fluid Phase Equilibria, 447, (2017) pp.39-71.

Magoulas, K. and Tassios, D. Thermophysical Properties of n-Alkanes from C1 to C20 and Their Prediction for Higher Ones. Fluid Phase Equilibria, 56, (1990) pp.119-140.

Martin, J. Equations of State – Applied Thermodynamics Symposium. Industrial & Engineering Chemistry, 59(12), (1967) pp.34-52.

Mathias, P., Naheiri, T., and Oh, E. A Density Correction for the Peng—Robinson Equation of State. Fluid Phase Equilibria, 47(1), (1989) pp.77-87.

Nojabaei, B., Johns, R., and Chu, L. Effect of Capillary Pressure on Phase Behavior in Tight Rocks and Shales. SPE Reservoir Evaluation & Engineering, 16(03), (2013) pp.281-289.

Oellrich, L., Plocker, U., Prausnitz, J., and Knapp, H. Equation-of-State Methods for Computing Phase Equilibria and Enthalpies. Int. Chem. Eng., 21(1), (1981) pp. 1-15.

Pedersen, K., Milter, J., and Sørensen, H. Cubic Equations of State Applied to HT/HP and Highly Aromatic Fluids. SPE Journal, 9(02), (2004) pp.186-192.

Péneloux, A., Rauzy, E., and Fréze, R. A Consistent Correction for Redlich-Kwong-Soave Volumes. Fluid Phase Equilibria, 8(1), (1982) pp.7-23.

Peng, D. and Robinson, D. A New Two-Constant Equation of State. Industrial & Engineering Chemistry Fundamentals, 15(1), (1976) pp.59-64.

Qi, Z., Liang, B., Deng, R., Du, Z., Wang, S., and Zhao, W. Phase Behavior Study in the Deep Gas-Condensate Reservoir with Low Permeability. In: SPE Europec/EAGE Annual Conference and Exhibition. London: Society of Petroleum Engineers (2007).

Qiu, X., Tan, S., Dejam, M., and Adidharma, H. Simple and accurate isochoric differential scanning calorimetry measurements: phase transitions for pure fluids and mixtures in nanopores. Physical Chemistry Chemical Physics, 21(1), (2018) pp.224-231.

Rachford, H. and Rice, J. Procedure for Use of Electronic Digital Computers in Calculating Flash Vaporization Hydrocarbon Equilibrium. Journal of Petroleum Technology, 4(10), (1952) pp.19-3.

Redlich, O. and Kwong, J. On the Thermodynamics of Solutions. V. An Equation of State. Fugacities of Gaseous Solutions. Chemical Reviews, 44(1), (1949) pp.233-244.

Rezaveisi, M., Sepehrnoori, K., Pope, G., and Johns, R. Thermodynamic Analysis of Phase Behavior at High Capillary Pressure. SPE Journal, 23(06), (2018) pp.1977-1990.

Sandoval, D., Yan, W., Michelsen, M., and Stenby, E. Influence of Adsorption and Capillary Pressure on Phase Equilibria inside Shale Reservoirs. Energy & Fuels, 32(3), (2018) pp.2819-2833.

Sandoval, D., Yan, W., Michelsen, M., and Stenby, E. Phase Envelope Calculations for Reservoir Fluids in the Presence of Capillary Pressure. In: SPE Annual Technical Conference and Exhibition. Houston: Society of Petroleum Engineers (2015).

Sandoval, D., Yan, W., Michelsen, M., and Stenby, E. The Phase Envelope of Multicomponent Mixtures in the Presence of a Capillary Pressure Difference. Industrial & Engineering Chemistry Research, 55(22), (2016) pp.6530-6538.

Shi, J., Li, H., and Pang, W. An Improved Volume Translation Strategy for PR EOS without Crossover Issue. Fluid Phase Equilibria. 470, (2018) pp.164-175.

Soave, G. Equilibrium Constants from a Modified Redlich-Kwong Equation of State. Chemical Engineering Science, 27(6), (1972) pp.1197-1203.

Sun, H. and Li, H. A New Three-Phase Flash Algorithm Considering Capillary Pressure in a Confined Space. Chemical Engineering Science. 193, (2019) pp.346-363.

Tan, S. and Piri, M. Equation-of-State Modeling of Associating-Fluids Phase Equilibria in Nanopores. Fluid Phase Equilibria, 405, (2015) pp.157-166.

Tsai, J. and Chen, Y. Application of a Volume-Translated Peng-Robinson Equation of State on Vapor-Liquid Equilibrium Calculations. Fluid Phase Equilibria, 145(2), (1998) pp.193-215.

Ungerer, P. and Batut, C. Prédiction des Propriétés Volumétriques des Hydrocarbures par une Translation de Volume Améliorée. Revue de l'Institut Français du Pétrole, 52(6), (1997) pp.609-623.

van der Waals, J.D. Continuity of the Gaseous and Liquid State of Matter (1873).

Wang, Y., Yan, B., and Killough, J. Compositional Modeling of Tight Oil Using Dynamic Nanopore Properties. In: SPE Annual Technical Conference and Exhibition. New Orleans: Society of Petroleum Engineers (2013).

Watson, P., Cascella, M., May, D., Salerno, S., and Tassios, D. Prediction of vapor Pressures and Saturated Molar Volumes with a Simple Cubic Equation of State: Part II: The van der Waals - 711 EOS. Fluid Phase Equilibria, 27, (1986) pp.35-52.Weinaug, C. and Katz, D. Surface Tensions of Methane-Propane Mixtures. Industrial & Engineering Chemistry, 35(2), (1943) pp.239-246.

Weinaug, C. and Katz, D. Surface Tensions of Methane-Propane Mixtures. Industrial & Engineering Chemistry, 35(2), (1943) pp.239-246.

Whitson, C. and Brulé, M. Phase Behavior. Richardson, TX: Henry L. Doherty Memorial Fund of AIME, Society of Petroleum Engineers (2000).

Wilson, G.M., A Modified Redlich-Kwong Equation of State, Application to General Physical Data Calculations. In: 65th National AIChE Meeting. Cleveland (1969).

Young, A.F., Pessoa, F.L.P., and Ahon, V.R.R. Comparison of Volume Translation and Co-Volume Functions Applied in the Peng-Robinson EOS for Volumetric Corrections. Fluid Phase Equilibria, 435, (2017) pp.73-87.

Young, T. An Essay on the Cohesion of Fluids. Philosophical Transactions of the Royal Society of London, 95, (1805) pp.65-87.

Zhang, Y., Lashgari, H., Di, Y., and Sepehrnoori, K. Capillary Pressure Effect on Phase Behavior of CO_2/Hydrocarbons in Unconventional Reservoirs. Fuel, 197, (2017) pp.575-582.

Zhong, J., Zhao, Y., Lu, C., Xu, Y., Jin, Z., Mostowfi, F., and Sinton, D. Nanoscale Phase Measurement for the Shale Challenge: Multicomponent Fluids in Multiscale Volumes. Langmuir, 34(34), (2018) pp.9927-9935.